Proceedings of the Third Lunar Science Conference
(Supplement 3, *Geochimica et Cosmochimica Acta*)
Vol. 3, pp. 2387–2395
The M.I.T. Press, 1972

Magnetic properties of Apollo 14 breccias and their correlation with metamorphism

W. A. GOSE
Lunar Science Institute, Houston, Texas 77058

G. W. PEARCE
Lunar Science Institute, Houston, Texas 77058 and
Department of Physics, University of Toronto

D. W. STRANGWAY
Geophysics Branch, NASA, Manned Spacecraft Center, Houston, Texas 77058

and

E. E. LARSON
Department of Geological Sciences, University of Colorado, Boulder, Colorado

Abstract—The magnetic properties of Apollo 14 breccias can be explained in terms of the grain size distribution of the interstitial iron which is directly related to the metamorphic grade of the sample. In samples 14049 and 14313 iron grains < 500 Å in diameter are dominant as evidenced by a Richter-type magnetic aftereffect and hysteresis measurements. Both samples are of lowest metamorphic grade. The medium metamorphic-grade sample 14321 and the high-grade sample 14312 both show a logarithmic time-dependence of the magnetization indicative of a wide range of relaxation times and thus grain sizes, but sample 14321 contains a stable remanent magnetization whereas sample 14312 does not. This suggests that small multidomain particles (< 1 μ) are most abundant in sample 14321 while sample 14312 is magnetically controlled by grains > 1 μ. The higher the metamorphic grade, the larger the grain size of the iron controlling the magnetic properties. Experiments on synthetic lunar glasses suggest that solid-state reduction during impact is an effective mechanism for producing the interstitial iron. It is therefore concluded that the remanent magnetization in the lunar breccias is of thermal origin and contemporaneous with the time of breccia formation.

INTRODUCTION

WITH THE RETURN OF the Apollo 14 rocks it has become necessary to examine closely the magnetization of breccias since most samples were of this type. As we have pointed out earlier (Gose *et al.*, 1972) the breccias offer the best hope of extending the record of the lunar magnetic field over a considerable portion of lunar history since igneous rocks seem to be restricted to the time between about 3 and 4 b.y. Before breccias can be used it must be demonstrated that they possess a stable magnetization which was acquired during the formation of the breccia.

Generally, the breccias show a pronounced viscous remanent magnetization (VRM), but it is often possible to isolate a component which is as stable as the magnetization which is typical of the igneous rocks (Doell *et al.*, 1970; Nagata and Carleton, 1970; Gose *et al.*, 1972). We have had the opportunity to examine four

breccias from the Apollo 14 mission and it seems possible now to draw some general conclusions as to the origin and nature of the magnetic properties and remanent magnetization of the breccias.

Viscous remanent magnetization of breccias 14049, 14312, 14313, and 14321

The time dependence of the magnetization is of two basic types. The first type is illustrated in Fig. 1. Samples 14049,28 and 14313,25 were exposed to a magnetic field of 2.5 Oe for 8 min. At time $t = 0$ the field was removed and the decay of the magnetization in a field-free space was measured as a function of time. This behavior can be explained in terms of a Richter-type aftereffect (e.g. Becker and Döring, 1939). In the Richter model, the relaxation times of the magnetic particles are assumed to be restricted to a finite range between, say, τ_1 (lower limit) and τ_2 (upper limit). This model has been successfully applied to several lunar breccias by Nagata and Carleton (1970) and by Gose *et al.* (1972). From these curves it is not possible to obtain the lower limit of the relaxation times τ_1. But the shape of the curve allows one to estimate the upper limit, τ_2, with considerable accuracy. For both samples shown in Fig. 1 this value lies between 100 and 1000 min.

According to Néel's theory (Néel, 1949) the relaxation times are related to grain size. Using values for iron, the equation can be written in the form

$$\log \tau = 2.68 \times 10^{18} H_{RC} \frac{v}{T} - 0.5 \log \frac{v}{T} - \log H_{RC} - 16.8$$

where H_{RC} is the remanence coercive force, v the volume of the grain, and T the absolute temperature. The value of the coercive force is a rather critical quantity in this equation. For spherical single-domain particles H_{RC} is determined by the crystalline anisotropy, and for iron the value is about 170 Oe, assuming that there is no significant

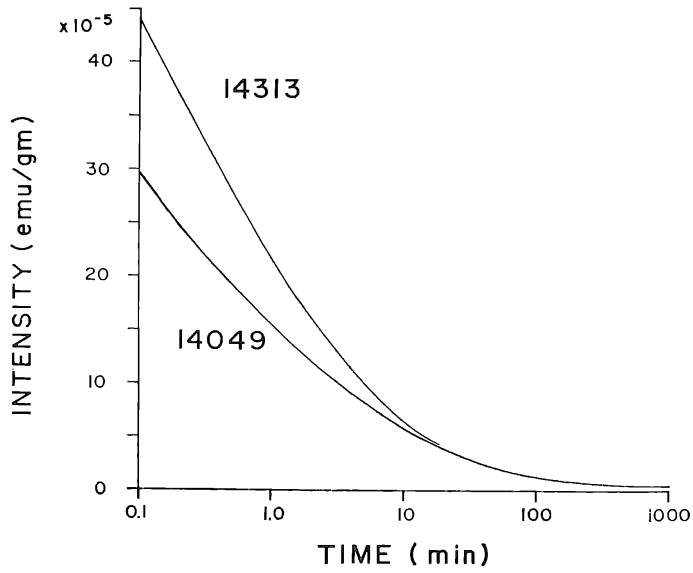

Fig. 1. Decay of VRM induced in samples 14049 and 14313 by a magnetic field of 2.5 Oe. Both samples were measured up to 1000 min.

strain. By adding a small amount of cobalt or nickel the value for H_{RC} decreases. If the particle deviates from sphericity, shape anisotropy becomes the dominant factor. For a prolate ellipsoid with an axial ratio larger than 1.1 the shape is the controlling factor for the coercive force. Figure 2 illustrates the dependence of the value of H_{RC} on the grain size for a given relaxation time and temperature. The vertical axis shows the diameter for a sphere with a volume equivalent to a prolate ellipsoid whose axial ratio is indicated along the curve. In this example the equivalent grain size can vary from about 120 Å to 270 Å depending on the possible range of H_{RC}. The precise value of this range is not of great importance considering that the lunar samples contain iron grains ranging in size up to 100 μ. It is, however, of theoretical interest in that the upper limit of the relaxation time coincides with the transition from superparamagnetic to single domain grains.

The experimentally determined value of the remanence coercive force is 460 Oe for sample 14313, which corresponds to a grain size of 185 Å for the transition from superparamagnetic to single-domain behavior. However, the value of 460 Oe has to be considered an average value for an assemblage of grains many of which will have considerably larger coercivities. This is evidenced by steady field demagnetization experiments such as shown in Fig. 3. The sample was given an isothermal remanent magnetization (IRM) in an 18 kilogauss field. Then a dc field was applied in the opposite direction. The figure shows the decrease of the IRM as a function of the applied dc field; a wide coercive force spectrum is clearly present, ranging from 0 to at least 2500 Oe. Thus it seems more realistic to use a larger value than 460 Oe for the remanence coercive force of the very small particles. Néel (1949) reports a value of about 1000 Oe for fine grains of iron, and the same value was observed by Bertaut (1949). Stephenson (1971) obtains a value of 1700 Oe for iron grains in the range 60–120 Å in lunar dust. If we adopt a value of 1000 Oe for the lunar breccias, a grain size of about 150 Å is obtained for the transition from superparamagnetic to single-domain behavior at room temperature.

In view of our later discussion the important observation is that breccia 14049

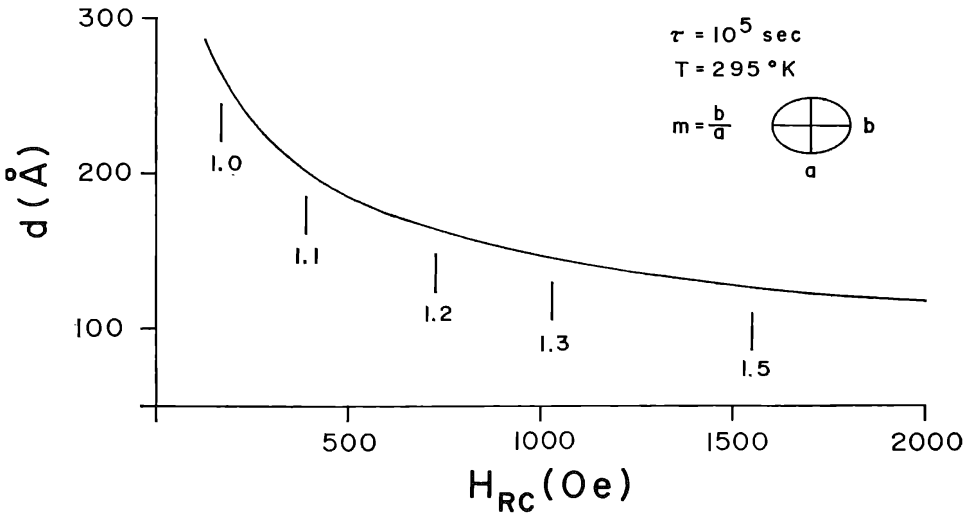

Fig. 2. Dependence of remanent coercivity H_{RC} on grain size.

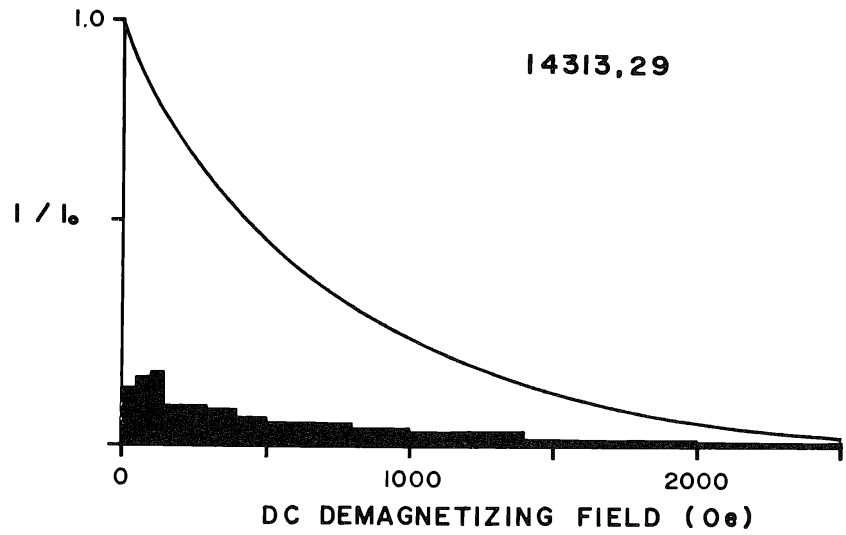

Fig. 3. D.C. demagnetization of IRM acquired in an 18-kilogauss field. Histogram indicates the portion of the intensity removed in a given interval.

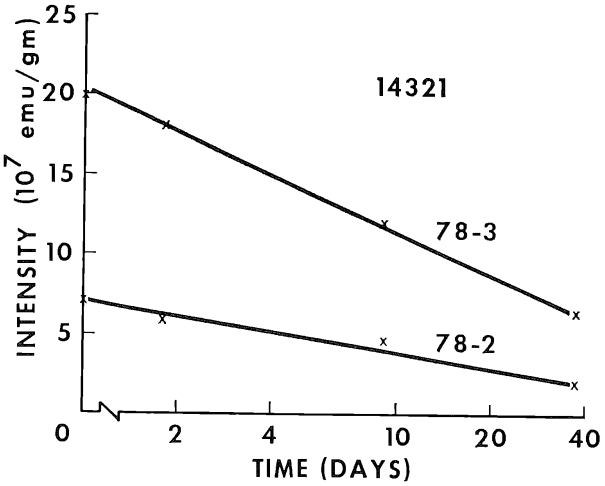

Fig. 4. Decay of natural remanent magnetization of samples 14321,78,2 and 14321,78,3 during storage in a field-free space.

and 14313 show a Richter-type aftereffect as the dominant VRM characteristic, and that this behavior is caused by superparamagnetic grains in the 100 Å range.

Two neighboring chips from breccia 14321 (78,1 and 78,3) show a different kind of VRM (Fig. 4). These samples were stored in a field-free space and measured over a 38-day period. The intensities decay linearly with the logarithm of time. One of these breccias was subjected to the same test as were the previous samples, and the log t relationship was found to be dominant down to 6 sec. Such behavior is observed when the relaxation times of the magnetic grains cover a time range which is very much larger than the duration of the experiment and is typical for multidomain grains (Néel, 1955). This sample has a stable magnetic remanence, however (Pearce *et al.*, this volume), which suggests that much of the magnetization is carried in grains less than a micron in size.

Sample 14312,07 exhibits a very weak response and a time dependence of magnetization which can be described by two log t functions after a 2.5 Oe field has been applied for 8 min (Fig. 5). But this sample differs from the other breccias in that no stable remanence could be isolated (Gose *et al.*, 1972; Pearce *et al.*, this volume). Upon AF demagnetization the directions of the natural remanence changed very erratically. Thus it is inferred that the magnetization of sample 14312 is controlled by rather large multidomain grains ($\gg 1$ μ).

Hysteresis measurements

In an earlier paper (Gose *et al.*, 1972) we described the usefulness of room temperature magnetization curves in determining the amount of iron present and its grain size distribution. A sample which has a magnetization curve which is almost linear (ramp-shaped) to saturation at 6000–7000 Oe and which has a small saturation remanence ($J_r/J_s = 0.01$ or less where J_r is the saturation remanence and J_s is the saturation magnetization) contains only iron grains whose magnetization is controlled by the demagnetizing field ($4\pi/3$ J_s for spherical grains). Equidimensional, multidomain particles have those properties. If the magnetization is measured on such a sample at higher temperatures (Fig. 6), the shape of the curve remains the same but saturation occurs at lower fields, since the demagnetizing field is proportional to the spontaneous magnetization of the grains. Superparamagnetic and stable single-domain particles, on the other hand, have quite different magnetization curves. Superparamagnetic grains have rounded curves which reach saturation in fields of less than 1000 Oe at room temperature if their radii are much above 20 Å. By definition they have no hysteresis, and the magnetization curves plotted against H/T can often be superimposed. An assemblage of stable single-domain grains, randomly oriented, shows rounded curves characterized by large hysteresis; for example, particles with uniaxial anisotropy have $J_r/J_s = 0.5$. The magnetization reaches approximate saturation in several thousand Oe for relatively equant grains (axial ratio b/a = 1.5 or less), but can approach 10,000 Oe for needlelike grains. (In the limit H_c = $2\pi J_s$ = 10,800 Oe.)

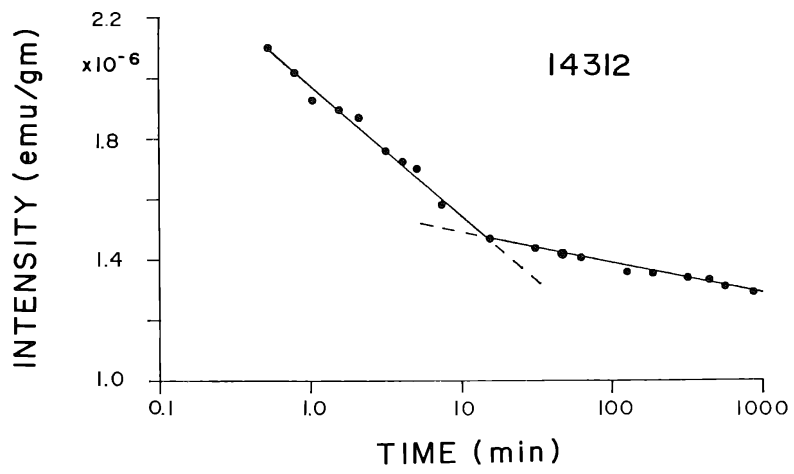

Fig. 5. Decay of VRM induced in sample 14312,7 by a magnetic field of 2.5 Oe.

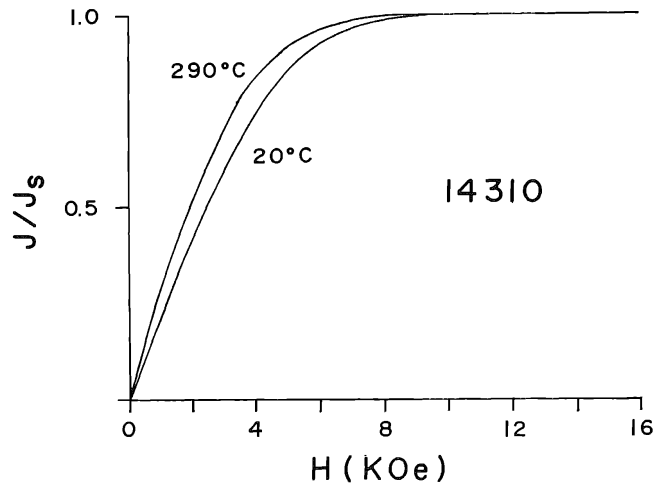

Fig. 6. Magnetization curves for igneous sample 14310 measured at 20°C and 290°C. These curves have been corrected for paramagnetic magnetization and then normalized to $J_s(T) = 1$.

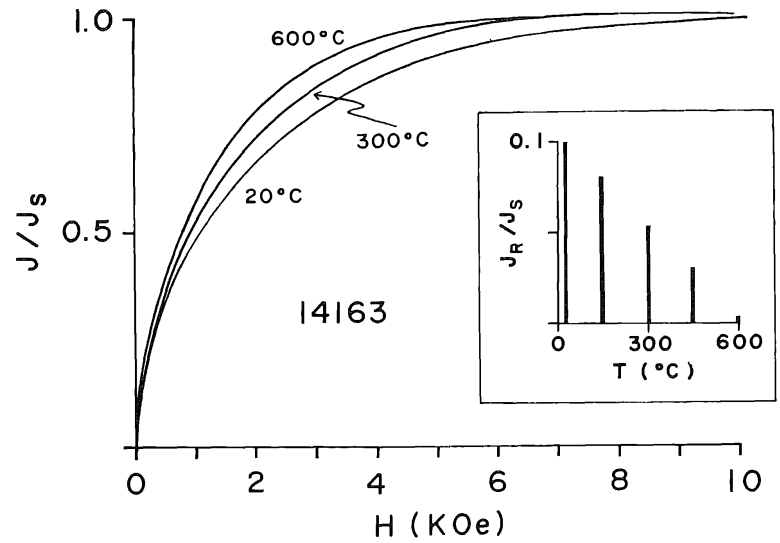

Fig. 7. Magnetization curves for soil 14163 measured at 20°C, 300°C, and 600°C. These curves have been corrected for paramagnetic magnetization and then normalized to $J_s(T) = 1$. (Inset) Histogram showing variation of ratio J_r/J_s with temperature for sample 14163.

Many igneous rocks and breccias which show log t-type after effect possess the simple ramp-shaped multidomain magnetization curve of Fig. 6, while the soils and those breccias which show a Richter-type aftereffect have complex curves, showing evidence of superparamagnetic and single-domain grains. For example, soil 14163 has a rounded curve (Fig. 7) with a J_r/J_s ratio of 0.1, suggesting that about 20 wt.% of the native iron grains in the sample are single-domain grains, assuming these to be uniaxial (that is, shape anisotropy predominates). The ratio decreases with increasing temperature, as the single-domain grains become superparamagnetic accord-

ing to the theory of Néel (1949). The increase in the quantity of superparamagnetic grains at high temperatures also explains the lack of superposition between the curves when plotted as J versus H/T (Fig. 8).

Optical studies

The different iron grain size distributions inferred from the VRM and hysteresis experiments can be seen in the optical microscope as well, although the limit of resolution is only about 0.25 μ. The examination of polished thin sections shows that most of the interstitial iron in sample 14312 is larger than 1 μ in size, whereas in sample 14321 grains below 1 μ are most abundant. The dominant size range in samples 14313 and 14049 lies at the limit of optical resolution, i.e. <0.25 μ. Most interesting is the

Table 1.

Sample no.	Metamorphic grade*	Mean Fe grain size	VRM behavior	Shape of hysteresis loop	J_r/J_s	Metallic Fe wt. %‡	Initial susceptibility ($\times 10^{-4}$ emu/g Oe)
14313	1	<500Å	Richter	Rounded	0.066	0.47	9.1
14049	1		Richter	Rounded	0.058	0.59	14.1
14047†	1		Richter				
14301†	2		Richter				
14063†	3	<1 μ	log t	Ramp	0.019	0.19	0.91
14321	4		log t				
14311†	5		log t				
14303†	6		log t				
14312	7	>1 μ	log t	Ramp	0.010	0.24	1.53
14310	Igneous			Ramp	0.019	0.10	0.57

* Warner, 1972.
† Nagata *et al.*, 1972.
‡ Determined from saturation magnetization curves.

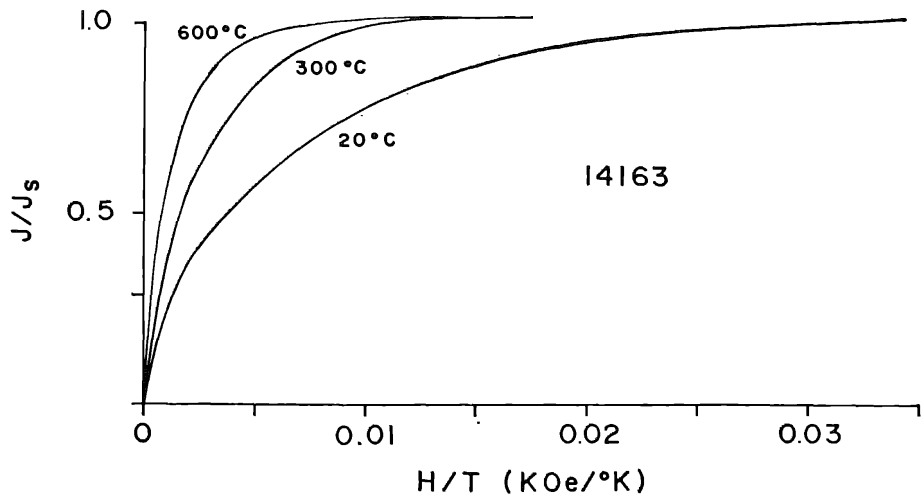

Fig. 8. Magnetization curve for soil with ratio H/T plotted on abscissa. The magnetization has been corrected for paramagnetic magnetization and then normalized to $J_s(T) = 1$.

fact that the latter two samples appear to contain less interstitial iron than samples 14321 and 14312, whereas the saturation magnetization clearly shows that the metallic iron concentration is considerably higher in 14049 and 14313 (Table 1). Since meteoritic iron makes up only a fraction of the metallic iron and is likely to be equally abundant in all the samples, it follows that most of the interstitial iron in 14049 and 14313 must be in the very fine grain size range ($\ll 0.25\ \mu$).

DISCUSSION

Based on these experiments it is possible to classify the Apollo 14 breccias into three groups. The first group, which is represented by samples 14049 and 14313, is magnetically dominated by superparamagnetic and single-domain iron grains. This is evidenced by a Richter-type magnetic aftereffect and a rounded hysteresis curve. The second group shows a VRM which decays linearly with a logarithm of time, has a ramp-shaped hysteresis curve, and carries a stable remanence. This behavior is caused by small multidomain grains. Sample 14321 belongs to this group. Samples 14312 is an example of the third group, which is similar to the second group in its VRM and hysteresis characteristics but differs from group 1 as well as group 2 in not having a stable remanent magnetization. Iron grains above 1 μ in size are most abundant in this sample. The different magnetic behavior is related to the metamorphic grade of the breccias. Warner (1972) classified the Apollo 14 breccias according to their metamorphic grade based on the abundance of matrix glass, glass clasts, and matrix texture. The lowest metamorphic grade (class 1) has a detrital matrix with abundant glass whereas the highest grade (class 8) is a glass-free breccia with a totally recrystallized matrix.

Table 1 presents variation of magnetic properties with increasing metamorphic grade, and summarizes our data on the Apollo 14 breccias, and includes some results from Nagata *et al.* (1972). For comparison the data on the igneous sample 14310 are shown as well. The magnetic properties correlate well with the metamorphic classification. Magnetically, the fundamental change is the increase in grain size of the interstitial iron from the 100 Å range in the lowest metamorphic-grade samples to grains larger than 1 μ in the highest-grade samples. All the magnetic characteristics can be attributed to this variation.

The correlation between the magnetic properties and the degree of metamorphism has been tested experimentally by Pearce and Williams (1972) with synthetic lunar glass powders. Upon heating to about 900°C in a reducing environment not too unlike those expected to occur in a large ejecta blanket, native iron of predominantly single-domain size is precipitated from the silicate melt. Heating to about 1000°C produces essentially only multidomain grains. In addition, the experiment shows that solid-state reduction during impact melting is an effective mechanism for producing the interstitial iron observed in the lunar breccias.

Since the interstitial iron is the main carrier of the stable remanent magnetization, we can conclude that this remanence must be of thermal origin and that it is contemporaneous with the formation of the breccia. Such an origin of the magnetization implies that the direction of magnetization should be uniform within a sample. The

three neighbouring chips of sample 14321 which we investigated yield similar directions (Pearce *et al.*, this volume). In addition, Hargraves and Dorety (1972) reported the same direction for another chip of the same sample which is separated from our chips by about 8 cm. It thus appears that the lunar breccias can indeed be used for reconstructing the history of the lunar magnetic field since they contain a stable magnetization (Gose *et al.*, 1972) which originated at the time of their formation.

Acknowledgments—Laboratory assistance in this work was ably provided by J. Love and E. Pahl of Lockheed Electronics Company. Financial support was provided to one of us (GWP) by the National Research Council of Canada and in part by the Lunar Science Institute. Financial support for WAG was provided by Contract No. NSR 09-051-001 between the National Aeronautics and Space Administration and the Universities Space Research Association. This paper constitutes the Lunar Science Institute contribution Number 93.

References

Becker R. and Döring W. (1939) *Ferromagnetismus*. Springer Verlag, Berlin.

Bertaut F. (1949) Champ coercitif et dimension cristalline. *Comptes Rendue* **229,** 417–419.

Doell R. R., Grommé C. S., Thorpe A. N., and Senftle F. E. (1970) Magnetic studies of Apollo 11 lunar samples. *Proc. Apollo 11 Lunar Sci. Conf., Geochim. Cosmochim. Acta* Suppl. 1, Vol. 3, pp. 2079–2102. Pergamon.

Gose W. A., Pearce G. W., Strangway D. W., and Larson E. E. (1972) On the applicability of lunar breccias for paleomagnetic interpretations. *The Moon*, in press.

Hargraves R. B. and Dorety N. (1972) Magnetic property measurements on several Apollo 14 rock samples (abstract). In *Lunar Science—III* (editor C. Watkins), pp. 357–359, Lunar Science Institute Contr. No. 88.

Nagata T. and Carleton B. J. (1970) Natural remanent magnetization and viscous magnetization of Apollo 11 lunar materials. *J. Geomag. Geoelectr.* **22,** 491–506.

Nagata T., Fisher R. M., Schwerer F. C., Fuller M. D., and Dunn J. R. (1972) Magnetism of Apollo 14 lunar materials (abstract). In *Lunar Science—III* (editor C. Watkins), pp. 573–575, Lunar Science Institute Contr. No. 88.

Néel L. (1949) Théorie du trainage magnétique des ferromagnétiques en grains fin avec application aux terres cuites. *Ann. Geophysique* **5,** 99–136.

Néel L. (1955) Some theoretical aspects of rock-magnetism. *Phil. Mag. Suppl.* **4,** 191–243.

Pearce G. W. and Williams R. J. (1972) Excess iron in lunar breccias and soils: A possible origin (abstract). EOS, *Trans. Amer. Geophys. Union* **53,** 360.

Stephenson A. (1971) Single domain grain distributions, II. The distribution of single domain iron grains in Apollo 11 lunar dust. *Phys. Earth Planet. Interiors* **4,** 361–369.

Warner J. L. (1972) Apollo 14 breccias: Metamorphic origin and classification (abstract). In *Lunar Science—III* (editor C. Watkins), pp. 782–784, Lunar Science Institute Contr. No. 88.